Extending the scope of poly(styrene)-block-poly(methyl methacrylate) for directed self assembly.

Thomas Bennett,[a,b] Kevin Pei,[a] Han Hao Cheng,[c] Kristofer J. Thurecht,[a,b] Kevin S. Jack,[d] and Idriss Blakey[a,b*]
*
[a] The University of Queensland, Australian Institute for Bioengineering and Nanotecnhology, Brisbane Qld Australia 4072; [b]The University of Queensland, Centre for Advanced Imaging, Brisbane Qld Australia 4072; [c] The University of Queensland, , Australian National Fabrication Facility, QLD Node, Brisbane Qld Australia 4072; [d] The University of Queensland Centre for Microscopy and Microanalysis, Brisbane Qld Australia 4072

ABSTRACT

Directed self-assembly (DSA) is a promising technique for extending conventional lithographic techniques by being able to print features with critical dimensions under 10 nm. The most widely studied block copolymer system is polystyrene-*block*-polymethyl methacrylate (PS-*b*-PMMA). The system is well understood in terms of its synthesis, properties and performance in DSA. However, PS-*b*-PMMA also has a number of limitations that impact on its performance and hence scope of application. The primary limitation is the low Flory-Huggins polymer-polymer interaction parameter (χ), which limits the size of features that can be printed by DSA. Another issue with block copolymers in general is that specific molecular weights need to be synthesized to achieve desired morphologies and feature sizes. We are exploring blending ionic liquid additiveswithPS-*b*-PMMAto increase the χ parameter. This allows smaller feature sizes to be accessed by PS-*b*-PMMA. Depending on the amount of additive it is also possible to tune the domain size and the morphology of the systems. These findings may expand the scope of PS-*b*-PMMA for DSA.

Keywords: ionic liquids, block copolymer, PS-b-PMMA, Chi parameter, Flory Huggins polymer-polymer interaction parameter

1. INTRODUCTION

Three key parameters that are used to measure the performance of photoresists are resolution, line edge roughness (LER) and sensitivity. It is well known that these three performance criteria are linked and thisrelationship is often described as the resolution-line edge roughness-sensitivity (RLS) trade-off. A key aim for the development of photoresists and associated processes is to simultaneously improve RLS. Many gains can be made by optimisation of resist formulations, although more disruptive technologies include the redesign of the resists and such approaches include: polymer bound PAG resists,[1-7] molecular glass resists[8-16] and chain scissioning resists.[17-26] In particular, polymer bound PAG resists have achieved a great deal of success as EUVL platforms, although improvements are still required for achieving the ITRS goals. Healing of LER following development is another approach that has led to significant improvements in LER.[27, 28] On the other hand, directed self assembly (DSA) of block copolymers is a technique that has demonstrated significant promise for achieving high resolution. DSA is a technique that brings together lithography (top-down) to fabricate patterns that guide the self assembly of diblock copolymers (bottom-up). The end result is ordered features with sub-lithographic resolution.[29-39] Block copolymers are made up of least two chemically-distinct polymer chains which are covalently linked. When the respective blocks are immiscible, arrays of highly-ordered nanostructures can form. The final morphology depends on the relative volume fraction of each block, the total molecular weight (N) and degree of immisciblity, i.e. the Flory-Huggins polymer-polymer interaction parameter, (χ). There are two main techniques for

i.blakey@uq.edu.au; www.aibn.uq.edu.au/a-prof-idriss-blakey

Alternative Lithographic Technologies VI, edited by Douglas J. Resnick, Christopher Bencher, Proc. of SPIE
Vol. 9049, 90490R · © 2014 SPIE · CCC code: 0277-786X/14/$18 · doi: 10.1117/12.2046296

carrying out DSA, namely chemo-epitaxy and grapho-epitaxy. Chemo-epitaxy relies on chemically patterning a substrate, where typically one of the components of the pattern preferentially interacts with one of the blocks and drives the ordering during self assembly. Grapho-epitaxy uses surface topography, e.g. a printed resist, to guide self assembly. Polystyrene-*block*-poly(methyl methacrylate), or PS-*b*-PMMA, is the most widely studied system, where directed self assembly of PS lines with a pitch of ~24 nm half pitch has been demonstrated.[40] There is also a significant body of knowledge relating to optimisation of processing and integration in to manufacture.

Nonetheless, PS-*b*-PMMA has some limitations in its scalability and compatibility for future nodes of fabrication because; (a) it has a small Flory-Huggins polymer-polymer interaction parameter ($\chi = 0.04$ [41]) limiting the ultimate resolution and (b) annealing temperatures are significantly higher than the glass temperature (T_g) of typical positive tone photoresists. As a result, next generation materials that can achieve better resolutions are being actively studied. Recently, we have reported our investigations of a high χ BCP, polystyrene-*b*-poly(DL-lactide) (PS-*b*-PLA) (χ = 0.217), which overcomes some of these issues. The high χ parameter enables much smaller domain sizes. Our initial efforts involved identifying the interfacial interactions of PS-*b*-PLA with substrates that were modified with a series of crosslinked mattes of statistical copolymers of PS and PMMA.[42] Lamellae as small as 8 nm could be achieved. Graphoepitaxy based DSA was also carried out with this system, where no resist freezing step was required a polyhydroxystyrene based photoresist template. The reason for this was because the spin coating solvent for the BCP was a non-solvent for the photoresist and the annealing temperature required to induce order was below the T_g of the photoresist.[43] While this system is promising, to achieve smaller feature sizes smaller than 8 nm may require the development of systems with even higher χ parameters. While there are a number of candidates that have been reported,[44-47] the disadvantage of such systems is that the development cycle can be long. For example, neutral surfaces may need to be identified and annealing conditions developed. Another option is solvent vapour annealing, in which solvent vapour is used to swell one or both blocks in a BCP and under the correct conditions can tune domain sizes and transition a system from one morphology to another.[48-52] These morphological changes can then be kinetically trapped by flash removal of the solvent from the system. However, a disadvantage is that this extra step requires extra equipment and strict control over the experimental parameters to achieve reproducible results.

The aim of this paper is to determine if additives can tune the properties of existing BCPs, i.e. PS-*b*-PMMA Figure 1 a). Ionic liquids (ILs) were the initial class of additives that were chosen. ILs are low melting point salts which generally consist of a large organic cation with low symmetry that is paired with an inorganic or organic polyatomic anion that is usually weakly basic and possesses a diffuse, or protected charge.[53] Ionic liquids are defined as salts with a melting point below 100 °C, but the majority of ionic liquids are liquid at or below room temperature.[54] The completely ionic composition of ILs endows them with a range of properties which makes them attractive candidates for both the replacement of many traditional organic solvents and as useful materials in a variety of applications. These properties include: non-flammibility, high chemical and thermal stability, high conducitvity, neglegible vapour pressure and relatively low toxicity compared to many other common organic solvents.[55, 56] In terms of use as an additive for BCP formulations the negligible vapour pressure, tunable solvent strength, chemical stability and thermal stability make ILs an attractive option. In this study we blend 1-ethyl-3-methylimidazolium [emim] bis(trifluoromethansulfonyl)amide [NTf2] (Figure 1b) with PS-b-PMMA and investigate the following questions 1) can $\chi_{PS\text{-}PMMA}$ be increased? 2) can the long period/pitch be tuned? and 3) can the morphology of a system be switched.? These questions are represented schematically in Figure 2, which shows how addition of ILs might help to traverse the BCP phase diagram.

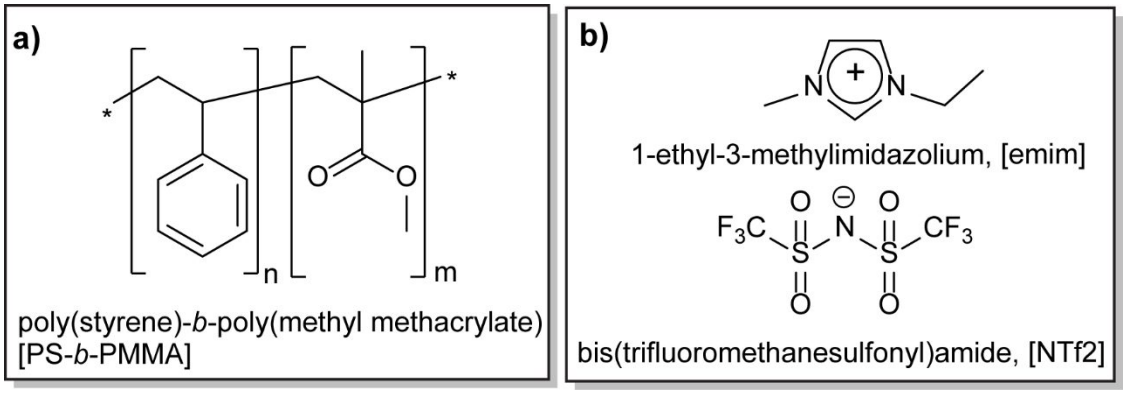

Figure 1. a) Structure of PS-b-PMMA.b) structure of the cation (top) and anion (bottom) of the ionic liquid.

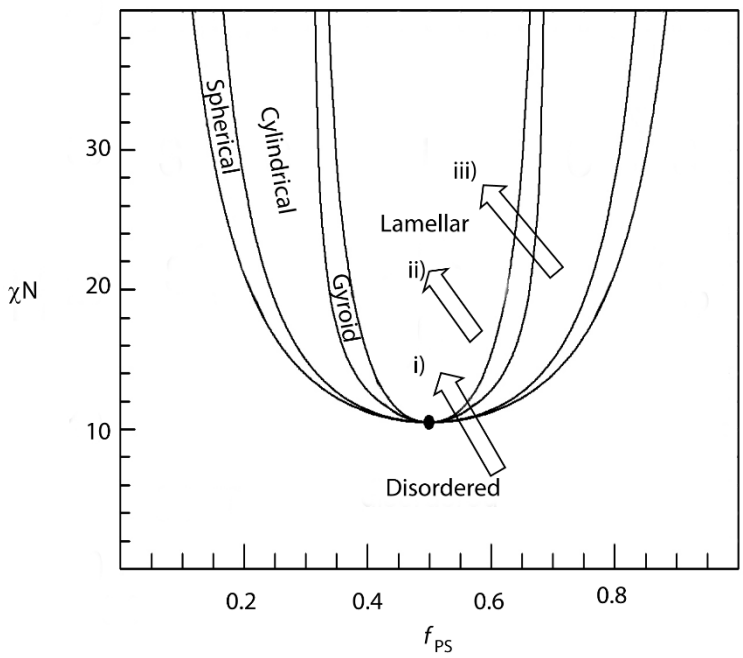

Figure 2. Block arrows show how addition of ionic liquids can be used to traverse the phase diagram for PS-b-PMMA. i) Transitioning from disordered to a lamellar morphology, ii) Tuning the pitch of lamellae, and iii) transitioning from a cylindrical to lamellar morphology.

2. EXPERIMENTAL

2.1 Polymer Materials and Characterization.

PS-*b*-PMMA block copolymers were purchased from Polymer Source Inc. and used without further purification. The dispersity of each block copolymer was assessed by GPC, and found to be ≤ 1.18. The PS-*b*-PMMA block copolymers are designated PS-*b*-PMMA (X–Y), where X and Y denote the number averaged molecular weights (M_n) in Da of the PS and PMMA blocks, respectively. The total M_n, dispersity ($Đ$), volume fraction of polystyrene (f_{PS}) and degree of polymerization (N) are given in Table 1.

Table 1. Block Copolymers Characteristics

Sample	**Total M_n (Da)**	**$Đ$**	**f_{PS}**	**N**
PS-b-PMMA (10k-b-10k)	20 000	1.18	0.53	196
PS-b-PMMA (38k–37k)	74 800	1.08	0.54	732
PS-b-PMMA (96k–36k)	132 000	1.11	0.75	1281

2.2 Ionic Liquid Synthesis and Purification.

1-ethyl-3-methylimidalzolium bis(trifluoromethanelsufonyl)amide, [emim][NTf_2], was synthesized via a metathesis reaction between equimolar amounts of [emim]Cl and Li[NTf_2] as described previously.[57, 58] Prior to use, the [emim][NTf_2] was further purified by stirring under high vacuum for several hours at 60 °C and subsequently stored under vacuum in a desiccator to avoid water absorption.

2.3 Silicon Wafer Surface Cleaning.

Silicon wafers were treated with an O_2 plasma generated in a reactive ion etcher, with a gas flow rate of 50 sccm, a chamber pressure of 50 mTorr, a power of 150 W and an exposure time of 60 s. Following plasma etching, each wafer

was soaked in methanol for 3 minutes, acetone for 3 minutes and finally in deionized water for 3 minutes. The wafers were subsequently dried in an oven for 10 minutes at 100 °C and then stored in a class P10000 clean room prior to use.

2.4 Preparation of PS-*r*-PMMA Underlayers on Silicon Wafers.

Statistical copolymers of polystyrene, poly(methyl methacrylate), and poly(glycidyl methacrylate) (PS-*stat*-PMMA-*stat*-PGMA) were prepared, spin coated onto silicon wafers, exposed to UV radiation and annealed on a hot plate as reported by Keen et al.,[42] with the exception that the statistical copolymers were spin coated from solutions of propylene glycol monomethyl ether acetate (PGMEA) instead of anisole. All films had thicknesses between 10-20 nm as determined via ellipsometry. The characteristics of the five statistical copolymers used to produce the underlayers are detailed in Table 2. All copolymers had 5 mole % of PGMA.

Table 2. Underlayer Characteristics

Underlayer	**Total M_n (kDa)**	***Đ***	**Mole % PS**
U1	23	1.26	75
U2	50	1.41	69
U3	30	1.29	65
U4	46	1.41	62
U5	62	1.58	52

2.5 Preparation of PS-*b*-PMMA/EMIM Tf_2N Bulk and Thin Films.

Thin films of PS-*b*-PMMA/EMIM Tf_2N were spin coated from PGMEA solutions onto a series of wafers coated with different underlayers. The desired thickness of the films studied was either 0.5 or 1 long periods, L_0, of the block copolymer being used, which was achieved by modifying the concentration of the block copolymer solutions and by adjusting the spin speed of the spin coater. Bulk films were prepared by solution casting onto Kapton films. Samples were annealed at 220 °C on a hotplate for 300 s, and where specified for a further 16 h at 200 °C under a nitrogen atmosphere.

2.6 Morphology Characterization of Bulk Films via SAXS.

The morphology of the block copolymer/ionic liquid composite was determined using small angle X-ray scattering (SAXS) on the Australian Synchrotron SAXS/WAXS beamline. The beamline was configured with an X-ray wavelength of λ = 1.512 Å and focused to a 235 μm horizontal × 140 μm vertical spot. Two dimensional scattering patterns were recorded on a Dectris - Pilatus 1M detector with an active area of 169 × 179 mm and a sample to detector distance of 3412 mm. The scattering patterns were then azimuthally integrated to give one-dimensional scattering data as intensity (I) vs wave vector ($q = 4\pi \sin(\theta/2)/\lambda$), where θ is the scattering angle (calibrated with silver behenate) and λ is the X-ray wavelength. Each scattering profile was also corrected for detector null signal, dark current and empty cell scattering using scatterBrain Analysis version 1.73 before morphological assignment.

2.7 Morphology Characterisation of Thin in Films by Grazing incidence small-angle X-ray scattering.

The morphology of each block copolymer/ionic liquid composite was determined using grazing incidence small angle X-ray scattering (SAXS) on the Australian Synchrotron SAXS/WAXS beamline. The beamline was configured with a photon energy of 12 keV, an X-ray wavelength of λ = 1.512 Å and focused to a 235 μm horizontal × 140 μm vertical spot. Two dimensional scattering patterns were recorded on a Dectris - Pilatus 1M detector with an active area of 169 × 179 mm and a sample to detector distance of 3431 mm. The scattering patterns were then azimuthally integrated to give one-dimensional scattering data as intensity (I) vs wave vector ($q = 4\pi \sin(\theta/2)/\lambda$), where θ is the scattering angle (calibrated with silver behenate) and λ is the X-ray wavelength. Each scattering profile was also corrected for detector null signal, dark current and bare silicon wafer scattering using scatterBrain Analysis version 1.73 before morphological assignment.

2.8 Scanning Electron Microscopy.

The morphologies of selected films were analyzed using a JEOL JSM-7800F scanning electron microscope (SEM). Films were mounted onto appropriate stubs using carbon tape, and stored in a vacuum oven at 50 °C overnight prior to analysis. In a typical setup, SEM micrographs were collected with a working distance of 2.7 mm while operating at 1 kV.

3. RESULTS AND DISCUSSION

3.1 Investigation of the effect of blended IL on the bulk morphology of PS-b-PMMA

The phase morphology of blends of PS-*b*-PMMA with varying amounts of the IL were studied using Synchrotron based SAXS. Figure 3a shows the SAXS profiles of PS-*b*-PMMA (10k-*b*-10k) with 0% and 5% of IL. The sample with 0% IL exhibited a disordered morphology. This was expected because χN for this system was approximately 8 at room temperature, which is below the minimum value of 10.5 that is predicted achieve phase separation of lamellae by mean field theory.[59] On the other hand, the sample with 5% IL, had a SAXS profile that was characteristic of a lamellar morphology, having Bragg peaks at 2 and 3 times q*. This indicated that for this particular formulation the ionic liquid was increasing the effective χ parameter by at least 31%. This was attributed to the IL being a good solvent for the PMMA chains and a poor solvent for the PS chains in the block copolymer, which decreases the miscibility of the PMMA and PS and increases the effective χ parameter. A similar effect has been observed for more conventional solvents that partition preferentially into one block, where it is possible to 'freeze' a morphology by flash annealing the system to evaporate the solvent. An advantage of blends of block copolymers with ILs is that the ILs do not evaporate under typical processing conditions used in directed self assembly, so do not require specialized vapor annealing chambers and precise amounts of the IL can be added during formulation of the BCP solutions. For example, the blends of PS-*b*-PMMA and emim NTf_2 could be annealed to 220 °C and the SAXS profile measured at that temperature remained unchanged. Perhaps the most distinct advantage is that by being able to achieve phase separation for systems that would usually be disordered, it should be possible to overcome the ~24 nm resolution limit of PS-*b*-PMMA. For example, the long period (pitch) of the PS-*b*-PMMA (10k-*b*-10k) with 5% IL was 20 nm. Further studies on systems with smaller block lengths is currently ongoing in our labs.

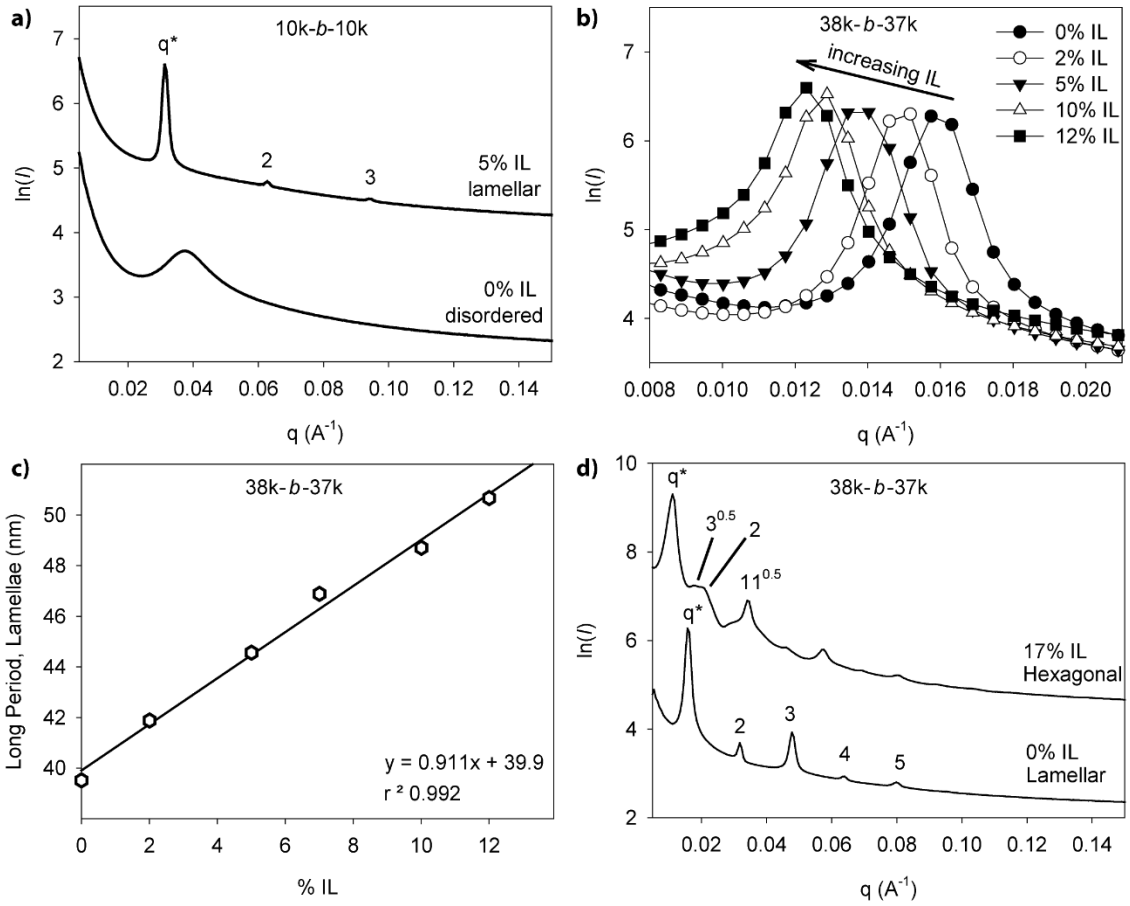

Figure 3 a) SAXS profiles of PS-*b*-PMMA (10k-*b*-10k) with 0% IL (bottom) and 5% IL (top). b) SAXS profiles focusing on the q* peak for a series of PS-*b*-PMMA (38k-*b*-37k)/IL blends for volume fractions of IL ranging 0-12%, iii) Plot showing relationship between the long period of PS-*b*-PMMA (38k-*b*-37k) and the IL content. d) SAXS profiles of PS-*b*-PMMA (38k-*b*-37k) for 0% IL and 17% IL.

Figure 3b shows a series of SAXS profiles, focusing on q*, for PS-*b*-PMMA (38k-*b*-37k) blended IL at concentrations varying from 0-12%. It can be seen that q* shifts to smaller q with increasing IL content. This indicates that the lamellar spacing was increasing as a function of IL content. This is quantified in Figure 3c, which shows that the long period of the lamellar morphology was approximately 39 nm for the neat BCP and this could be tuned up to 50.6 nm (~30%) by blending up to 12 % ionic liquid. In this case the long period could be incremented by about 0.9 nm per percent of IL in the system. This change in spacing could be attributed to swelling of the PMMA domain with increasing amounts of IL. Importantly for DSA applications, this demonstrates that the pitch of a given BCP can be tuned by simply incorporating an IL into the formulation. For example, a specific advantage may be that a BCP of a given molecular weight could be tuned such that it can be used for a wider range of pitches, perhaps reducing the need for extensive libraries of BCPs to cater to different pitch requirements.

Figure 3d shows the SAXS profiles of PS-*b*-PMMA (38k-*b*-37k) with 0% and 17% IL. The sample with no IL exhibits the characteristic profile for a lamellar morphology, whereas, the sample with 17% IL exhibits a hexagonal (cylindrical) morphology. This demonstrates that the morphology can transition when a sufficient volume fraction of IL is added, which may also be useful for some applications of DSA.

3.2 Investigation of the effect of blended IL on the thin film morphology and interfacial properties of PS-b-PMMA

It is well known that that the balance of interactions that each block has with the substrate and air interface can have a significant effect on the orientation of domains in thin films. For example, if the substrate preferentially interacts with

one of the blocks, then for a BCP that has a lamellar morphology the domains can orient parallel to the substrate. On the other hand, if substrate has non-preferential interactions with both blocks then the domains orient perpendicular to the substrate. A concern when blending an additive, such as an IL, into the BCP is that the surface energetics may change drastically, meaning that new compositions for 'neutral' underlayers may need to be identified. To determine whether blending of IL has an effect, PS-*b*-PMMA (38k-*b*-37k) with 20% IL was spin coated onto underlayers comprised of statistical copolymers of PS and PMMA that had PS compositions ranging from 52-75%. From our previous studies for this particular type of underlayer, this range encompassed the neutral window for PS-*b*-PMMA.[60] Figure 3 shows low resolution (20 × 20 μm field of view) AFM images for three underlayers, Figure 3a 69% PS, Figure 3b 65% PS and Figure 3c 62% PS. When the underlayer with 69% PS was used (Figure 3a), dewetting of the film was observed, which was attributed to the surface having poor interactions with both blocks. For the underlayer with 65% PS a relatively featureless film was observed, apart from some particulate contaminants. Finally, for the 62% underlayer a number of raised features were observed, which were characteristic of one block preferentially interacting with the substrate in a film that had a thickness that was incommensurate with the long period of the block copolymer.[61, 62] Qualitative analysis of these images suggested that the 65% PS may be a neutral surface for the PS-*b*-PMMA (38k-*b*-37k) with 20% IL. To investigate the morphology of the thin film further the PS-*b*-PMMA (38k-*b*-37k) with 20% IL on the 65% PS underlayer was analyzed using grazing incidence small angle X-ray scattering and a 2D scattering profile is shown in Figure 4a. In the profile, 2nd and 3rd order Bragg peaks are evident at integer multiples of q*. These peaks are more evident in the sector average shown in Figure 4b. This result confirms that the lamellae are oriented perpendicular to the substrate and that the 65% PS under layer can act as a neutral layer to blends of IL with PS-*b*-PMMA

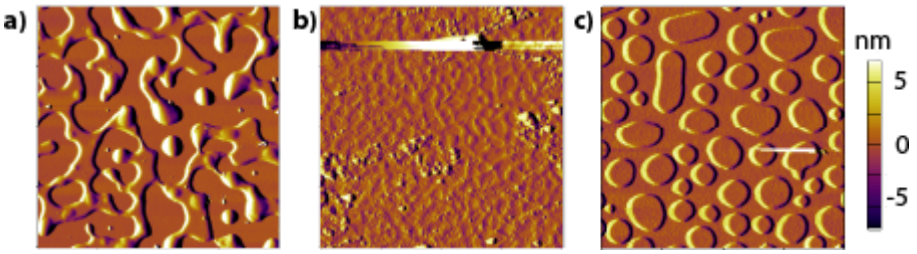

Figure 4 AFM micrographs of PS-*b*-PMMA (38k-*b*-37k) doped with 20% IL on three different underlayers, a) 69% PS, b) 65% PS and c) 62% PS.

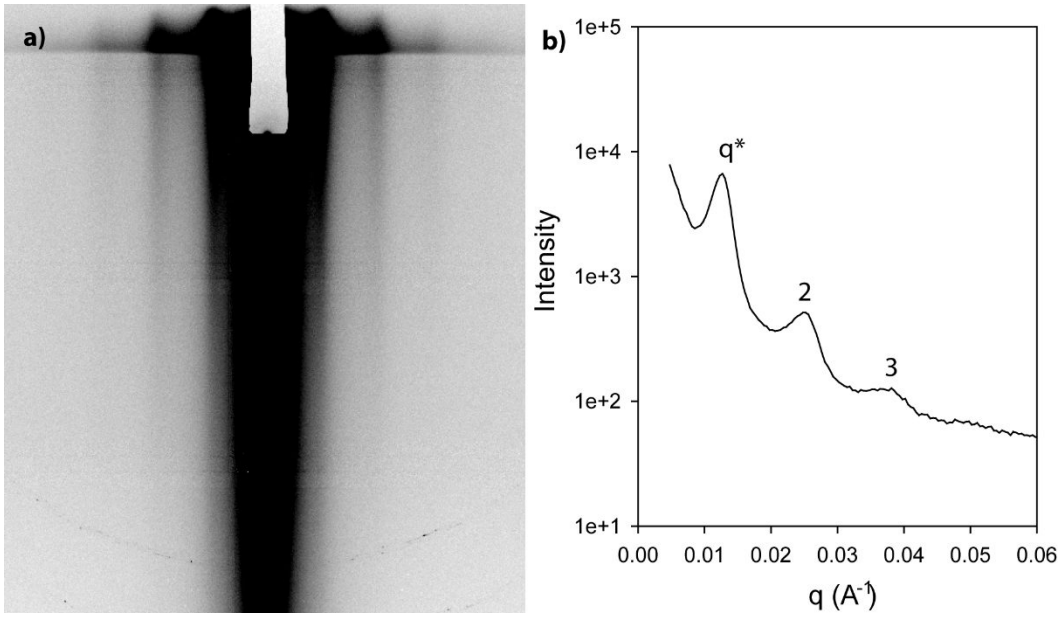

Figure 5 a) 2D GISAXS scattering profile for a thin film of PS-*b*-PMMA (38k-*b*-37k) doped with 20% IL on an underlayer containing 65% PS. b) Sector averaged 1D GISAXS profile. Both exhibit the characteristic Bragg peaks for lamellae oriented perpendicular to the substrate.

Having identified neutral surfaces for the blends of IL with BCP, experiments to demonstrate the tunability of the pitch and morphology in the thin film were conducted. Figure 6a shows high resolution SEM images of PS-*b*-PMMA (38k-*b*-37k) with 0% (left) and 25% (right) IL. In both cases a fingerprint pattern could be observered that was characteristic of lamellae oriented perpendicular to the substrate. It could also be seen that the samples with 0% IL had a number of cylinder-like defects, but these are not evident in the sample formulated with 25% IL. This indicates that defectivity may be lower for IL containing systems, although more systematic analysis is required to prove this. The insets of the SEM images show fast Fourier transforms (FFTs) that were calculated from the SEM images, which allowed the long period to be estimated. The sample with 0% IL had a peak at 39 nm, while sample formulated with 25% ionic liquid had a peak at 45 nm, confirming that the pitch of the lamellae could be tuned by introducing IL into the BCP formulation. However, the increase observed was significantly less than for the bulk films (Figure 2), i.e. a 6 nm change in the long period corresponds to a bulk sample with approximately 5.5 % IL. In addition, it would be expected that for a blend with 25% IL, the morphology should transition to a cylindrical/hexagonal morphology. One possible explanation for this difference is that the ionic liquid is partitioning into the underlayer, which is a statistical copolymer of styrene and methyl methacrylate. Partitioning of ionic liquid into the underlayer may also explain why the same underlayer acts as a neutral layer for formulations with 0% and 25% IL.

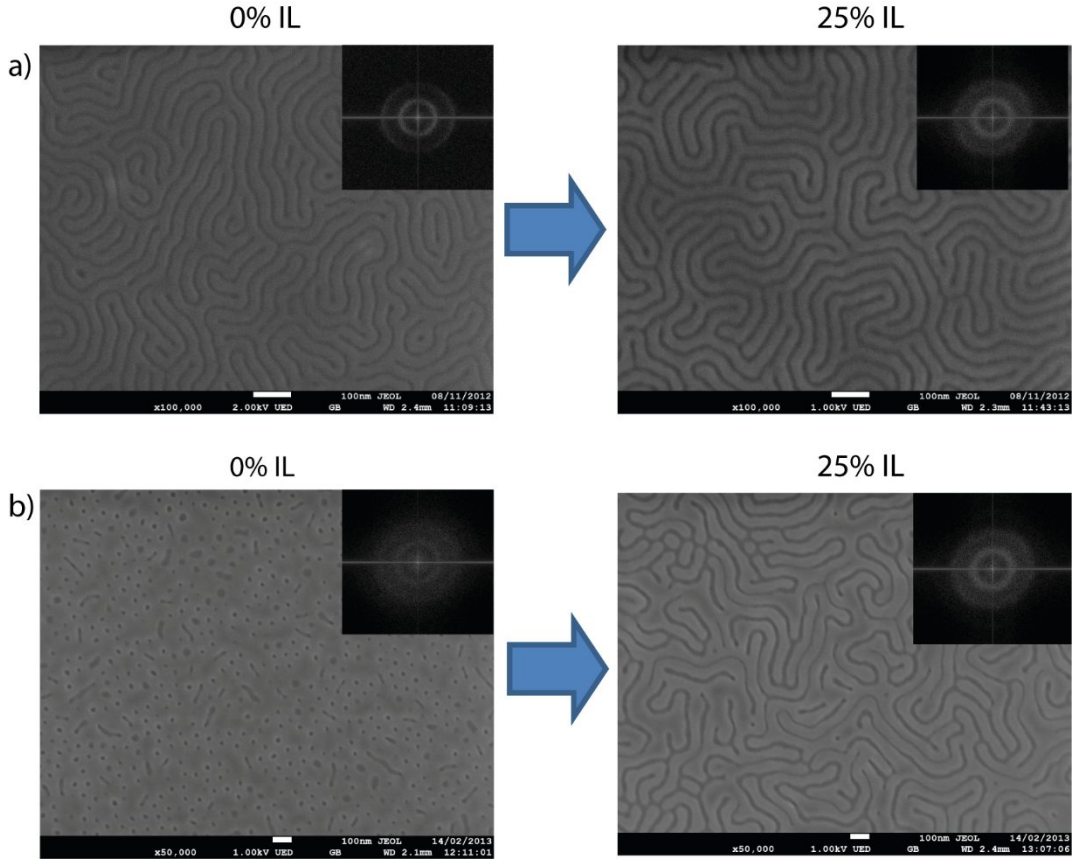

Figure 6 High resolution SEM of a) of thin films of neat PS-*b*-PMMA (38k-*b*-37k) [left] and of PS-*b*-PMMA (38k-*b*-37k) doped with 25% IL [right], b) of thin films of neat PS-*b*-PMMA (96k-*b*-36k) [left] and of PS-*b*-PMMA (96k-*b*-36k) doped with 25% IL. All samples used an underlayer that had a 65% PS content. The insets to the SEMs is the FFT calculated from the SEM images.

Finally we sought to determine if thethin film morphology of a BCP could be transformed by addition of IL. Figure 6b shows the high resolution SEMs of PS-*b*-PMMA (96k-*b*-36k) thin films with 0% and 25%. In the absence of IL a cylindrical/hexagonal morphology could be observed, while the formulation with 25% IL has transitioned to a lamellar morphology. The FFTs shown as insets confirm this.

4. CONCLUSIONS,,

This study has investigated the changes that occur to the bulk and thin film morphology of PS-*b*-PMMA when it is blended with varying amounts of an ionic liquid (IL), 1-ethyl-3-methylimidalzolium bis(trifluoromethanelsufonyl)amide (emim NTf_2). It was found that small amounts of IL could increase the effective parameter and could induce order for low molecular weight systems which undoped have χN values less than 10.5. In addition, it was demonstrated that in the bulk it was possible to tune the long period (pitch) of lamellae and transition from one morphology to another, simply by adding different amounts of IL. In terms of thin films containing 0- 25% IL, it was demonstrated that lamella oriented perpendicular to the substrate could be obtained using the same underlayer, i.e. a neutral underlayer optimized for PS-*b*-PMMA with no added IL. Finally, it was demonstrated that tuning of the long period and transitioning of morphologies could also be achieved in thin films. The favorable physical properties of ionic liquids, which include negligible vapour pressure and excelllent thermal stability mean that they can be formulated with BCPs in solution, spin coated and undergo high temperature annealing steps. This can all be achieved without conducting additional processing steps and does not require new equipment, which makes the appoach outlined in this study amenable to integration into current preproduction processing steps that have been developed by the industry.

5. ACKNOWLEDGEMENTS

Experiments were carried out in part at the Centre for Microscopy and Microanalysis (CMM), The University of Queensland (UQ); Queensland node of the Australian Microscopy and Microanalysis Research Facility, UQ; and the Australian National Fabrication Facility (ANFF) (Qld-node). This research was supported in part under the *Australian Research Councils* Discovery Project Scheme (DP140103118) and Future Fellowship Scheme (FT100100721, for IB) as well as UQs Postgraduate Research Award (for TB).

REFERENCES

[1] Wu, H., and Gonsalves, K.E., "Novel Positive-Tone Chemically Amplified Resists with Photoacid Generator in the Polymer Chains," Adv. Mater., 13(9), 670-672 (2001).
[2] Wu, H., and Gonsalves, K.E., "Preparation of a Photoacid Generating Monomer and Its Application in Lithography," Adv. Funct. Mater., 11(4), 271-276 (2001).
[3] Wang, M., Gonsalves, K.E., Wang, Y., and Roberts, J.M., "Novel anionic photoacid generators (PAGs) and corresponding PAG bound polymers," Macromol. Rapid Commun., 27, 1590-1595 (2006).
[4] Wang, M., Jarnagin, N.D., Lee, C.-T., Henderson, C.L., Wang, Y., Roberts, J.M., and Gonsalves, K.E., "Novel polymeric anionic photoacid generators (PAGs) and corresponding polymers for 193 nm lithography," J. Mater. Chem., 16, 3701-3707 (2006).
[5] Gonsalves, K.E., Wang, M., Lee, C.-T., Wang, Y., Tapia-Tapia, M., Batina, N., and Henderson, C.L., "Novel chemically amplified resists incorporating anionic photoacid generator functional groups for sub-50-nm half-pitch lithography," J. Mater. Chem., 19, 2797-2802 (2009).
[6] Gronheid, R., Vaglio, P.A., Rathsack, B., Hooge, J., Scheer, S., Nafus, K., Shite, H., and Kitano, J., "Resolution-linewidth roughness-sensitivity performance tradeoffs for an extreme ultraviolet polymer bound photoacid generator resist," J. Micro/Nanolithogr., MEMS, MOEMS, 10, 013017/013011-013017/013018 (2011).
[7] Thackeray, J.W., Jain, V., Coley, S., Christianson, M., Arriola, D., LaBeaume, P., Kang, S.-J., Wagner, M., Sung, J.W., and Cameron, J., "Optimization of polymer-bound PAG (PBP) for 20nm EUV lithography," J. Photopolym. Sci. Technol., 24, 179-183 (2011).
[8] Chang, S.W., Ayothi, R., Bratton, D., Yang, D., Felix, N., Cao, H.B., Deng, H., and Ober, C.K., "Sub-50 nm feature sizes using positive tone molecular glass resists for EUV lithography," J. Mater. Chem., 16, 1470-1474 (2006).
[9] Dai, J., Chang, S.W., Hamad, A., Yang, D., Felix, N., and Ober, C.K., "Molecular Glass Resists for High-Resolution Patterning," Chem. Mater., 18, 3404-3411 (2006).
[10] De, S.A., Forman, D., and Ober, C.K., "Molecular glass resists for EUV lithography," Proc. SPIE-Int. Soc. Opt. Eng., 6153, 615341/615341-615341/615310 (2006).
[11] Felix, N.M., De, S.A., Luk, C.M.Y., and Ober, C.K., "Dissolution phenomena of phenolic molecular glass photoresist films in supercritical CO2," J. Mater. Chem., 17, 4598-4604 (2007).

[12] De, S.A., Felix, N.M., and Ober, C.K., "Molecular glass resists as high-resolution patterning materials," Adv. Mater., 20, 3355-3361 (2008).
[13] Kang, S., Lavery, K., Choi, K.-W., Prabhu, V.M., Wu, W.-L., Lin, E., De, S.A., Felix, N., and Ober, C., "A comparison of the reaction-diffusion kinetics between model-EUV polymer and molecular-glass photoresists," Proc. SPIE, 6923, 692317/692311-692317/692312 (2008).
[14] Lawson, R.A., Yeh, W.-M., and Henderson, C.L., "Bond contribution model for the prediction of glass transition temperature in polyphenol molecular glass resists," J. Vac. Sci. Technol., B: Microelectron. Nanometer Struct.--Process., Meas., Phenom., 27, 3004-3009 (2009).
[15] Tanaka, S., Murakami, M., Fukushima, K., Kawano, N., Uenoyama, Y., Ito, K., Ohno, H., and Matsumoto, N., "Adamantane-based molecular glass resist for 193-nm lithography," Proc. SPIE, 7273, 72732M/72731-72732M/72738 (2009).
[16] Okumura, A., Funaki, Y., Takaragi, A., Okamoto, K., Tsutsumi, K., Inoue, K., Itaya, R., Ikura, K., and Iguchi, Y., "Novel molecular glass photoresist materials for next-generation lithography," Proc. SPIE, 7639, 76392E/76391-76392E/76398 (2010).
[17] Lawrie, K.J., Blakey, I., Blinco, J.P., Cheng, H.H., Gronheid, R., Jack, K.S., Pollentier, I., Leeson, M.J., Younkin, T.R., and Whittaker, A.K., "Chain scission resists for extreme ultraviolet lithography based on high performance polysulfone-containing polymers," J. Mater. Chem., 21, 5629-5637 (2011).
[18] Lawrie, K., Blakey, I., Blinco, J., Gronheid, R., Jack, K., Pollentier, I., Leeson, M.J., Younkin, T.R., and Whittaker, A.K., "Extreme ultraviolet (EUV) degradation of poly(olefin sulfone)s: Towards applications as EUV photoresists," Radiat. Phys. Chem., 80(2), 236-241 (2011).
[19] Chen, L., Goh, Y.-K., Lawrie, K., Chuang, Y., Piscani, E., Zimmerman, P., Blakey, I., and Whittaker, A.K., "Polysulfone based non-CA resists for 193 nm immersion lithography: Effect of increasing polymer absorbance on sensitivity," Radiat. Phys. Chem., 80(2), 242-247 (2011).
[20] Yu, A., Liu, H., Blinco, J.P., Jack, K.S., Leeson, M., Younkin, T.R., Whittaker, A.K., and Blakey, I., "Patterning of Tailored Polycarbonate Based Non-chemically-amplified Resists using Extreme Ultraviolet Lithography," Macromol. Rapid Commun., 31(16), 1449–1455 (2010).
[21] Chen, L., Goh, Y.-K., Lawrie, K., Smith, B., Montgomery, W., Zimmerman, P., Blakey, I., and Whittaker, A., "Non-chemically amplified resists for 193-nm immersion lithography: influence of absorbance on performance," Proc. SPIE, 7639, 763953/763901-763953/763909 (2010).
[22] Blakey, I., Yu, A., Blinco, J., Jack, K.S., Liu, H., Leeson, M., Yeuh, W., Younkin, T., and Whittaker, A.K., "Polycarbonate Based Non-chemically Amplified Photoresists for Extreme Ultraviolet Lithography," Proc. SPIE, 7636, 763635 (2010).
[23] Whittaker, A.K., Blakey, I., Blinco, J., Jack, K.S., Lawrie, K., Liu, H., Yu, A., Leeson, M., Yeuh, W., and Younkin, T., "Development of polymers for non-CAR resists for EUV lithography," *Proc. SPIE*, 7273, 727321 (2009).
[24] Blakey, I., Chen, L., Goh, Y.-K., Lawrie, K., Chuang, Y.-M., Piscani, E., Zimmerman, P.A., and Whittaker, A.K., "Non-CA resists for 193 nm immersion lithography: effects of chemical structure on sensitivity," *Proc. SPIE*, 7273, 72733X (2009).
[25] Jack, K., Liu, H., Blakey, I., Hill, D., Wang, Y., Cao, H., Leeson, M., Denbeaux, G., Waterman, J., and Whittaker, A., "The rational design of polymeric EUV resist materials by QSPR modelling," Proc. SPIE, 6519, 65193Z (2007).
[26] Chen, L., Goh, Y.K., Cheng, H.H., Smith, B.W., Xie, P., Montgomery, W., Whittaker, A.K., and Blakey, I., "Aqueous developable dual switching photoresists for nanolithography," Journal of Polymer Science Part A: Polymer Chemistry, 50(20), 4255–4265 (2012).
[27] Chuang, Y.-M., Jack, K.S., Cheng, H.H., Whittaker, A.K., and Blakey, I., "Using Directed Self Assembly of Block Copolymer Nanostructures to Modulate Nanoscale Surface Roughness: Towards a Novel Lithographic Process," Adv. Funct. Mater., 23(2), 173-183 (2013).
[28] Chuang, Y.-M., Cheng, H.-H., Jack, K., Whittaker, A., and Blakey, I., "Healing LER using directed self assembly: treatment of EUVL resists with aqueous solutions of block copolymers," Proc. SPIE, 8680(Alternative Lithographic Technologies V), 868009/868001-868009/868010 (2013).
[29] Black, C.T., Ruiz, R., Breyta, G., Cheng, J.Y., Colburn, M.E., Guarini, K.W., Kim, H.C., and Zhang, Y., "Polymer self assembly in semiconductor microelectronics," IBM J. Res. Dev., 51, 605-633 (2007).
[30] Cheng, J.Y., Ross, C.A., Smith, H.I., and Thomas, E.L., "Templated self-assembly of block copolymers: top-down helps bottom-up," Adv. Mater., 18(19), 2505-2521 (2006).

[31] Stoykovich, M.P., Kang, H., Daoulas, K.C., Liu, G., Liu, C.-C., de Pablo, J.J., Mueller, M., and Nealey, P.F., "Directed Self-Assembly of Block Copolymers for Nanolithography: Fabrication of Isolated Features and Essential Integrated Circuit Geometries," ACS Nano, 1(3), 168-175 (2007).
[32] Detcheverry, F.A., Nealey, P.F., and de, P.J.J., "Directed Assembly of a Cylinder-Forming Diblock Copolymer: Topographic and Chemical Patterns," Macromolecules, 43, 6495-6504 (2010).
[33] Herr, D.J.C., "Directed block copolymer self-assembly for nanoelectronics fabrication," J. Mater. Res., 26, 122-139 (2011).
[34] Jeong, J.-W., Park, W.-I., Kim, M.-J., Ross, C.A., and Jung, Y.-S., "Highly Tunable Self-Assembled Nanostructures from a Poly(2-vinylpyridine-b-dimethylsiloxane) Block Copolymer," Nano Lett., 11, 4095-4101 (2011).
[35] Kim, B.J., Given-Beck, S., Bang, J., Hawker, C.J., and Kramer, E.J., "Importance of End-Group Structure in Controlling the Interfacial Activity of Polymer-Coated Nanoparticles," Macromolecules, 40, 1796-1798 (2007).
[36] Kriksin, Y.A., Khalatur, P.G., Neratova, I.V., Khokhlov, A.R., and Tsarkova, L.A., "Directed Assembly of Block Copolymers by Sparsely Patterned Substrates," J. Phys. Chem. C, 115, 25185-25200 (2011).
[37] Park, S.-M., Liang, X., Harteneck, B.D., Pick, T.E., Hiroshiba, N., Wu, Y., Helms, B.A., and Olynick, D.L., "Sub-10 nm Nanofabrication via Nanoimprint Directed Self-Assembly of Block Copolymers," ACS Nano, 5, 8523–8531 (2011).
[38] Tada, Y., Yoshida, H., Ishida, Y., Hirai, T., Bosworth, J.K., Dobisz, E., Ruiz, R., Takenaka, M., Hayakawa, T., and Hasegawa, H., "Directed Self-Assembly of POSS Containing Block Copolymer on Lithographically Defined Chemical Template with Morphology Control by Solvent Vapor," Macromolecules, 45, 292-304 (2012).
[39] Tiron, R., Chevalier, X., Couderc, C., Pradelles, J., Bustos, J., Pain, L., Navarro, C., Magnet, S., Fleury, G., and Hadziioannou, G., "Optimization of block copolymer self-assembly through graphoepitaxy: a defectivity study," J. Vac. Sci. Technol., B: Nanotechnol. Microelectron.: Mater., Process., Meas., Phenom., 29, 06F206/201-206F206/208 (2011).
[40] Cheng, J.Y., Sanders, D.P., Truong, H.D., Harrer, S., Friz, A., Holmes, S., Colburn, M., and Hinsberg, W.D., "Simple and Versatile Methods To Integrate Directed Self-Assembly with Optical Lithography Using a Polarity-Switched Photoresist," ACS Nano, 4(8), 4815-4823 (2010).
[41] Russell, T.P., Hjelm, R.P., and Seeger, P.A., "Temperature dependence of the interaction parameter of polystyrene and poly(methyl methacrylate)," Macromolecules, 23(3), 890-893 (1990).
[42] Keen, I., Yu, A., Cheng, H.-H., Jack, K.S., Nicholson, T.M., Whittaker, A.K., and Blakey, I., "Control of the Orientation of Symmetric Poly(styrene)-block-poly(d,l-lactide) Block Copolymers Using Statistical Copolymers of Dissimilar Composition," Langmuir, 28(45), 15876–15888 (2012).
[43] Keen, I., Cheng, H.-H., Yu, A., Jack, K.S., Younkin, T.R., Leeson, M.J., Whittaker, A.K., and Blakey, I., "Behavior of Lamellar Forming Block Copolymers under Nanoconfinement: Implications for Topography Directed Self-Assembly of Sub-10 nm Structures," Macromolecules 47(1), 276-283 (2014).
[44] Jung, Y.S., and Ross, C.A., "Orientation-Controlled Self-Assembled Nanolithography Using a Polystyrene−Polydimethylsiloxane Block Copolymer," Nano Lett., 7(7), 2046-2050 (2007).
[45] Chai, J., and Buriak, J.M., "Using Cylindrical Domains of Block Copolymers To Self-Assemble and Align Metallic Nanowires," ACS Nano, 2(3), 489-501 (2008).
[46] Park, S., Lee, D.H., Xu, J., Kim, B., Hong, S.W., Jeong, U., Xu, T., and Russell, T.P., "Macroscopic 10-Terabit–per–Square-Inch Arrays from Block Copolymers with Lateral Order," Science, 323(5917), 1030-1033 (2009).
[47] Park, S.-M., Liang, X., Harteneck, B.D., Pick, T.E., Hiroshiba, N., Wu, Y., Helms, B.A., and Olynick, D.L., "Sub-10 nm Nanofabrication via Nanoimprint Directed Self-Assembly of Block Copolymers," ACS Nano, 5(11), 8523-8531 (2011).
[48] Park, S., Kim, B., Xu, J., Hofmann, T., Ocko, B.M., and Russell, T.P., "Lateral Ordering of Cylindrical Microdomains Under Solvent Vapor," Macromolecules, 42(4), 1278-1284 (2009).
[49] Kim, S.H., Misner, M.J., Xu, T., Kimura, M., and Russell, T.P., "Highly Oriented and Ordered Arrays from Block Copolymers via Solvent Evaporation," Adv. Mater., 16(3), 226-231 (2004).
[50] Cavicchi, K.A., Berthiaume, K.J., and Russell, T.P., "Solvent annealing thin films of poly(isoprene-b-lactide)," Polymer, 46(25), 11635-11639 (2005).
[51] Vayer, M., Hillmyer, M.A., Dirany, M., Thevenin, G., Erre, R., and Sinturel, C., "Perpendicular orientation of cylindrical domains upon solvent annealing thin films of polystyrene-b-polylactide," Thin Solid Films, 518(14), 3710-3715 (2010).
[52] Cushen, J.D., Wan, L., Pandav, G., Mitra, I., Stein, G.E., Ganesan, V., Ruiz, R., Grant Willson, C., and Ellison, C.J., "Ordering poly(trimethylsilyl styrene-block-D,L-lactide) block copolymers in thin films by solvent annealing using a mixture of domain-selective solvents," Journal of Polymer Science Part B: Polymer Physics, 52(1), 36-45 (2014).

[53] Forsyth, S.A., Pringle, J.M., and MacFarlane, D.R., "Ionic Liquids-An Overview," Aust. J. Chem., 57(2), 113-119 (2004).
[54] Wasserscheid, P., and Welton, T.: 'Ionic Liquids in Synthesis' (2003. 2003)
[55] Welton, T., "Room-Temperature Ionic Liquids. Solvents for Synthesis and Catalysis," Chem. Rev. (Washington, DC, U. S.), 99(8), 2071-2084 (1999).
[56] McFarlane, D.R., Sun, J., Golding, J., Meakin, P., and Forsyth, M., "High conductivity molten salts based on the imide ion," Electrochim. Acta, 45(8–9), 1271-1278 (2000).
[57] Burrell, A.K., Sesto, R.E.D., Baker, S.N., McCleskey, T.M., and Baker, G.A., "The large scale synthesis of pure imidazolium and pyrrolidinium ionic liquids," Green Chem., 9(5), 449-454 (2007).
[58] Bonhôte, P., Dias, A.-P., Papageorgiou, N., Kalyanasundaram, K., and Grätzel, M., "Hydrophobic, Highly Conductive Ambient-Temperature Molten Salts†," Inorg. Chem., 35(5), 1168-1178 (1996).
[59] Leibler, L., "Theory of Microphase Separation in Block Copolymers," Macromolecules, 13(6), 1602-1617 (1980).
[60] Cheng, H., Yu, A., Keen, I., Chuang, Y., Jack, K., Leeson, M., Younkin, T., Blakey, I., and Whittaker, A., "Electron-beam induced freezing of an aromatic based EUV resist: A robust template for directed self assembly of block copolymers," Nanotechnology, IEEE Transactions on, 11(6), 1140-1147 (2012).
[61] In, I., La, Y.-H., Park, S.-M., Nealey, P.F., and Gopalan, P., "Side-Chain-Grafted Random Copolymer Brushes as Neutral Surfaces for Controlling the Orientation of Block Copolymer Microdomains in Thin Films," Langmuir, 22(18), 7855-7860 (2006).
[62] Suh, H.S., Kang, H., Liu, C.-C., Nealey, P.F., and Char, K., "Orientation of Block Copolymer Resists on Interlayer Dielectrics with Tunable Surface Energy," Macromolecules, 43(1), 461-466 (2009).